Outage Performance of Two-Way Relay Non-Orthogonal Multiple Access Systems

Xinwei Yue*, Yuanwei Liu†, Shaoli Kang*, Arumugam Nallanathan†, and Yue Chen†
*Beihang University, Beijing, China
† Queen Mary University of London, London, UK

***Abstract*—This paper investigates a two-way relay non-orthogonal multiple access (TWR-NOMA) system, where two groups of NOMA users exchange messages with the aid of one half-duplex (HD) decode-and-forward (DF) relay. Since the signal-plus-interference-to-noise ratios (SINRs) of NOMA signals mainly depend on effective successive interference cancellation (SIC) schemes, imperfect SIC (ipSIC) and perfect SIC (pSIC) are taken into consideration. To characterize the performance of TWR-NOMA systems, we derive closed-form expressions for both exact and asymptotic outage probabilities of NOMA users' signals with ipSIC/pSIC. Based on the results derived, the diversity order and throughput of the system are examined. Numerical simulations demonstrate that: 1) TWR-NOMA is superior to TWR-OMA in terms of outage probability in low SNR regimes; and 2) Due to the impact of interference signal (IS) at the relay, error floors and throughput ceilings exist in outage probabilities and ergodic rates for TWR-NOMA, respectively.**

I. Introduction

With the purpose to meet the requirements of future radio access, the design of non-orthogonal multiple access (NOMA) technologies is important to enhance spectral efficiency and user access [1]. The major viewpoint of NOMA is to superpose multiple users by sharing radio resources (i.e., time/frequencey/code) over different power levels [2–4]. Then the desired signals are detected by exploiting the successive interference cancellation (SIC) [5]. Very recently, the integration of cooperative communication with NOMA has been widely discussed in many treaties [6–9]. Cooperative NOMA has been proposed in [6], where the user with better channel condition acts as a decode-and-forward (DF) relay to forward information. With the objective of improving energy efficiency, the application of simultaneous wireless information and power transfer (SWIPT) to the nearby user was investigated where the locations of NOMA users were modeled by stochastic geometry [7]. Considering the impact of imperfect channel state information (CSI), the authors in [8] investigated the performance of amplify-and-forward (AF) relay for downlink NOMA networks, where the exact and tight bounds of outage probability were derived. To further enhance spectrum efficiency, the performance of full-duplex (FD) cooperative NOMA was characterized in terms of outage behaviors [9], where user relaying was capable of switching operation between FD and HD mode.

Above existing treaties on cooperative NOMA are all based on one-way relay scheme, where the messages are delivered in only one direction, (i.e., from the BS to the relay or user destinations). As a further advance, two-way relay (TWR) technique introduced in [10] has attracted remarkable interest as it is capable of boosting spectral efficiency. The basic idea of TWR systems is to exchange information between two nodes with the help of a relay. In [11], the authors studied the outage behaviors of DF relay with perfect and imperfect CSI conditions. In terms of CSI and system state information (SSI), the system outage behavior was investigated for two-way full-duplex (FD) DF relay on different multi-user scheduling schemes [12].

Motivated by the above two technologies, we focus our attentions on the outage behaviors of TWR-NOMA systems, where two groups of NOMA users exchange messages with the aid of a relay node using DF protocol. Considering both perfect SIC (pSIC) and imperfect SIC (ipSIC), we derive the closed-form expressions of outage probabilities for users' signals. To provide valuable insights, we further derive the asymptotic outage probabilities of users' signals and obtain the diversity orders. We show that the outage performance of TWR-NOMA is superior to TWR-OMA in the low signal-to-noise ratio (SNR) regime. We demonstrate that the outage probabilities for TWR-NOMA converge to error floors due to the effect of interference signal (IS) at the relay. We confirm that the use of pSIC is incapable of overcoming the zero diversity order for TWR-NOMA. Additionally, we discuss the system throughput in delay-limited transmission mode.

II. System Model

We consider a two-way relay NOMA communication scenario which consists of one relay R, two pairs of NOMA users $G_1 = \{D_1, D_2\}$ and $G_2 = \{D_3, D_4\}$. Assuming that D_1 and D_3 are the nearby users in group G_1 and G_2, respectively, while D_2 and D_4 are the distant users in group G_1 and G_2, respectively. The exchange of information between user groups G_1 and G_2 is facilitated via the assistance of a decode-and-forward (DF) relay with two antennas, namely A_1 and A_2. User nodes are equipped with single antenna and can transmit the superposed signals [13, 14]. In addition, we assume that the direct links between two pairs of users are inexistent due to the effect of strong shadowing. Without loss of generality, all the wireless channels are modeled to be independent quasi-static block Rayleigh fading channels and disturbed by additive white Gaussian noise with mean power N_0. We denote that h_1, h_2, h_3 and h_4 are denoted as the complex channel coefficient of $D_1 \leftrightarrow R$, $D_2 \leftrightarrow R$, $D_3 \leftrightarrow R$ and $D_4 \leftrightarrow R$ links, respectively. The channel power gains

978-1-5386-3180-5/18/$31.00 ©2018 IEEE

$|h_1|^2$, $|h_2|^2$, $|h_3|^2$ and $|h_4|^2$ are assumed to be exponentially distributed random variables (RVs) with the parameters Ω_i, $i \in \{1,2,3,4\}$, respectively. It is assumed that the perfect CSIs of NOMA users are available at R for signal detection.

During the first slot, the pair of NOMA users in G_1 transmit the signals to R just as uplink NOMA. Due to R is equipped with two antennas, when the R receives the signals from the pair of users in G_1, it will suffer from interference signals from the pair of users in G_2. More precisely, the observation at R for A_1 is given by

$$y_{R_{A_1}} = h_1\sqrt{a_1 P_u}x_1 + h_2\sqrt{a_2 P_u}x_2 + \varpi_1 I_{R_{A_2}} + n_{R_{A_1}}, \tag{1}$$

where $I_{R_{A_2}}$ denotes IS from A_2 with $I_{R_{A_2}} = (h_3\sqrt{a_3 P_u}x_3 + h_4\sqrt{a_4 P_u}x_4)$. $\varpi_1 \in [0,1]$ denotes the impact levels of IS at R. P_u is the normalized transmission power at user nodes. x_1, x_2 and x_3, x_4 are the signals of D_1, D_2 and D_3, D_4, respectively, i.e, $\mathbb{E}\{x_1^2\} = \mathbb{E}\{x_2^2\} = \mathbb{E}\{x_3^2\} = \mathbb{E}\{x_4^2\} = 1$. a_1, a_2 and a_3, a_4 are the corresponding power allocation coefficients. Note that the efficient uplink power control is capable of enhancing the performance of the systems considered, which is beyond the scope of this paper. $n_{R_{A_j}}$ denotes the Gaussian noise at R for A_j, $j \in \{1,2\}$.

Similarly, when R receives the signals from the pair of users in G_2, it will suffer from interference signals from the pair of users in G_1 as well and then the observation at R is given by

$$y_{R_{A_2}} = h_3\sqrt{a_3 P_u}x_3 + h_4\sqrt{a_4 P_u}x_4 + \varpi_1 I_{R_{A_1}} + n_{R_{A_2}}, \tag{2}$$

where $I_{R_{A_1}}$ denotes the interference signals from A_1 with $I_{R_{A_1}} = (h_1\sqrt{a_1 P_u}x_1 + h_2\sqrt{a_2 P_u}x_2)$.

Applying the NOMA protocol, R first decodes D_l's information x_l by the virtue of treating x_t as IS. Hence the received signal-to-interference-plus-noise ratio (SINR) at R to detect x_l is given by

$$\gamma_{R\to x_l} = \frac{\rho|h_l|^2 a_l}{\rho|h_t|^2 a_t + \rho\varpi_1(|h_k|^2 a_k + |h_r|^2 a_r) + 1}, \tag{3}$$

where $\rho = \frac{P_u}{N_0}$ denotes the transmit SNR, $(l,k) \in \{(1,3),(3,1)\}$, $(t,r) \in \{(2,4),(4,2)\}$.

After SIC is carried out at R for detecting x_l, the received SINR at R to detect x_t is given by

$$\gamma_{R\to x_t} = \frac{\rho|h_t|^2 a_t}{\varepsilon\rho|g|^2 + \rho\varpi_1(|h_k|^2 a_k + |h_r|^2 a_r) + 1}, \tag{4}$$

where $\varepsilon = 0$ and $\varepsilon = 1$ denote the pSIC and ipSIC employed at R, respectively. Due to the impact of ipSIC, the residual IS is modeled as Rayleigh fading channels [15] denoted as g with zero mean and variance Ω_I.

In the second slot, the information is exchanged between G_1 and G_2 by the virtue of R. Therefore, just like the downlink NOMA, R transmits the superposed signals $(\sqrt{b_1 P_r}x_1 + \sqrt{b_2 P_r}x_2)$ and $(\sqrt{b_3 P_r}x_3 + \sqrt{b_4 P_r}x_4)$ to G_2 and G_1 by A_2 and A_1, respectively. b_1 and b_2 denote the power allocation coefficients of D_1 and D_2, while b_3 and b_4 are the corresponding power allocation coefficients of D_3 and D_4, respectively. P_r is the normalized transmission power at R. In particular, to ensure the fairness between users in G_1 and G_2, a higher power should be allocated to the distant user who has the worse channel conditions. Hence we assume that $b_2 > b_1$ with $b_1 + b_2 = 1$ and $b_4 > b_3$ with $b_3 + b_4 = 1$. Note that the fixed power allocation coefficients for two groups' NOMA users are considered. Relaxing this assumption will further improve the performance of systems and should be concluded in our future work.

According to NOMA protocol, SIC is employed and the received SINR at D_k to detect x_t is given by

$$\gamma_{D_k\to x_t} = \frac{\rho|h_k|^2 b_t}{\rho|h_k|^2 b_l + \rho\varpi_2|h_k|^2 + 1}, \tag{5}$$

where $\varpi_2 \in [0,1]$ denotes the impact level of IS at the user nodes. Then D_k detects x_l and gives the corresponding SINR as follows:

$$\gamma_{D_k\to x_l} = \frac{\rho|h_k|^2 b_l}{\varepsilon\rho|g|^2 + \rho\varpi_2|h_k|^2 + 1}. \tag{6}$$

Furthermore, the received SINR at D_t to detect x_r is given by

$$\gamma_{D_r\to x_t} = \frac{\rho|h_r|^2 b_t}{\rho|h_r|^2 b_l + \rho\varpi_2|h_r|^2 + 1}. \tag{7}$$

From above process, the exchange of information is achieved between the NOMA users for G_1 and G_2.

III. Outage Probability

In this section, the performance of TWR-NOMA is characterized in terms of outage probability.

1) Outage Probability of x_l: In TWR-NOMA, the outage events of x_l are explained as follow: i) R cannot decode x_l correctly; ii) The information x_t cannot be detected by D_k; and iii) D_k cannot detect x_l, while D_k can first decode x_t successfully. To simplify the analysis, the complementary events of x_1 are employed to express its outage probability. Hence the outage probability of x_l with ipSIC for TWR-NOMA is expressed as

$$\begin{aligned} P_{x_l}^{ipSIC} =& 1 - \Pr\left(\gamma_{R\to x_l} > \gamma_{th_l}\right) \\ &\times \Pr\left(\gamma_{D_k\to x_t} > \gamma_{th_t}, \gamma_{D_k\to x_l} > \gamma_{th_l}\right), \end{aligned} \tag{8}$$

where $\varepsilon = 1$, $\varpi_1 \in [0,1]$ and $\varpi_2 \in [0,1]$. $\gamma_{th_l} = 2^{2R_l} - 1$ with R_l being the target rate at D_k to detect x_l and $\gamma_{th_t} = 2^{2R_t} - 1$ with R_t being the target rate at D_k to detect x_t.

The following theorem provides the outage probability of x_l for TWR-NOMA.

Theorem 1. *The closed-form expression for the outage probability of x_l for TWR-NOMA with ipSIC is given by*

$$\begin{aligned} P_{x_l}^{ipSIC} = 1 - e^{-\frac{\beta_l}{\Omega_l}} \prod_{i=1}^{3} \lambda_i \left(\frac{\Phi_1\Omega_l}{\Omega_l\lambda_1+\beta_l} - \frac{\Phi_2\Omega_l}{\Omega_l\lambda_2+\beta_l} \right. \\ \left. + \frac{\Phi_3\Omega_l}{\Omega_l\lambda_3+\beta_l}\right) \left(e^{-\frac{\theta_l}{\Omega_k}} - \frac{\varepsilon\tau_l\rho\Omega_I}{\Omega_k + \varepsilon\rho\tau_l\Omega_I} e^{-\frac{\theta_l(\Omega_k+\varepsilon\rho\tau_l\Omega_I)}{\varepsilon\tau_l\rho\Omega_I\Omega_k} + \frac{1}{\varepsilon\rho\Omega_I}}\right), \end{aligned} \tag{9}$$

where $\varepsilon = 1$. $\lambda_1 = \frac{1}{\rho a_t \Omega_t}$, $\lambda_2 = \frac{1}{\rho \varpi_1 a_k \Omega_k}$ *and* $\lambda_3 = \frac{1}{\rho \varpi_1 a_r \Omega_r}$. $\beta_l = \frac{\gamma_{th_l}}{\rho a_l}$. $\Phi_1 = \frac{1}{(\lambda_2-\lambda_1)(\lambda_3-\lambda_1)}$, $\Phi_2 = \frac{1}{(\lambda_3-\lambda_2)(\lambda_2-\lambda_1)}$ *and* $\Phi_3 = \frac{1}{(\lambda_3-\lambda_1)(\lambda_3-\lambda_2)}$. $\theta_l \triangleq \max(\tau_l, \xi_t)$. $\tau_l = \frac{\gamma_{th_l}}{\rho\left(b_l - \varpi_2 \gamma_{th_l}\right)}$ *with* $b_l > \varpi_2 \gamma_{th_l}$ *and* $\xi_t = \frac{\gamma_{th_t}}{\rho\left(b_t - b_l \gamma_{th_t} - \varpi_2 \gamma_{th_t}\right)}$ *with* $b_t > (b_l + \varpi_2)\gamma_{th_t}$.

Proof: See Appendix A. ∎

Corollary 1. *Based on* (9)*, for the special case* $\varepsilon = 0$*, the outage probability of* x_1 *for TWR-NOMA with pSIC is given by*

$$P_{x_l}^{pSIC} = 1 - e^{-\frac{\beta_l}{\Omega_l} - \frac{\theta_l}{\Omega_k}} \prod_{i=1}^{3} \lambda_i \left(\frac{\Phi_1 \Omega_l}{\Omega_l \lambda_1 + \beta_l} - \frac{\Phi_2 \Omega_l}{\Omega_l \lambda_2 + \beta_l} + \frac{\Phi_3 \Omega_l}{\Omega_l \lambda_3 + \beta_l} \right). \quad (10)$$

2) Outage Probability of x_t: Based on NOMA principle, the complementary events of outage for x_t have the following cases. One of the cases is that R can first decode the information x_l and then detect x_t. Another case is that either of D_k and D_r can detect x_t successfully. Hence the outage probability of x_t can be expressed as

$$P_{x_t}^{ipSIC} = 1 - \Pr\left(\gamma_{R \to x_t} > \gamma_{th_t}, \gamma_{R \to x_l} > \gamma_{th_l}\right) \times \Pr\left(\gamma_{D_k \to x_t} > \gamma_{th_t}\right) \Pr\left(\gamma_{D_r \to x_t} > \gamma_{th_t}\right), \quad (11)$$

where $\varepsilon = 1$, $\varpi_1 \in [0, 1]$ and $\varpi_2 \in [0, 1]$.

The following theorem provides the outage probability of x_t for TWR-NOMA.

Theorem 2. *The closed-form expression for the outage probability of* x_t *with ipSIC is given by*

$$P_{x_t}^{ipSIC} = 1 - \frac{e^{-\frac{\beta_l}{\Omega_l} - \beta_t \varphi_t - \frac{\xi}{\Omega_k} - \frac{\xi}{\Omega_r}}}{\varphi_t \Omega_t \left(1 + \varepsilon \beta_t \rho \varphi_t \Omega_I\right)\left(\lambda_2' - \lambda_1'\right)} \prod_{i=1}^{2} \lambda_i' \times \left(\frac{\Omega_l}{\beta_l + \beta_t \Omega_1 \varphi_t + \Omega_l \lambda_1'} - \frac{\Omega_l}{\beta_l + \beta_t \Omega_1 \varphi_t + \Omega_l \lambda_2'} \right), \quad (12)$$

where $\varepsilon = 1$. $\lambda_1' = \frac{1}{\rho \varpi_1 a_k \Omega_k}$ *and* $\lambda_2' = \frac{1}{\rho \varpi_1 a_r \Omega_r}$. $\beta_t = \frac{\gamma_{th_t}}{\rho a_t}$, $\varphi_t = \frac{\Omega_l + \rho \beta_l a_t \Omega_t}{\Omega_l \Omega_t}$.

Proof: See Appendix B. ∎

Corollary 2. *For the special case, substituting* $\varepsilon = 0$ *into* (12)*, the outage probability of* x_2 *for TWR-NOMA with pSIC is given by*

$$P_{x_t}^{pSIC} = 1 - \frac{e^{-\frac{\beta_l}{\Omega_l} - \beta_t \varphi_t - \frac{\xi}{\Omega_k} - \frac{\xi}{\Omega_r}}}{\varphi_t \Omega_t \left(\lambda_2' - \lambda_1'\right)} \prod_{i=1}^{2} \lambda_i' \times \left(\frac{\Omega_l}{\beta_l + \beta_t \Omega_l \varphi_t + \Omega_l \lambda_1'} - \frac{\Omega_l}{\beta_l + \beta_t \Omega_l \varphi_t + \Omega_l \lambda_2'} \right). \quad (13)$$

3) Diversity Order Analysis: To obtain deeper insights for TWR-NOMA systems, the asymptotic analysis are presented in high SNR regimes based on the derived outage probabilities. The diversity order is defined as [16, 17]

$$d = -\lim_{\rho \to \infty} \frac{\log\left(P_{x_i}^{\infty}(\rho)\right)}{\log \rho}, \quad (14)$$

where $P_{x_i}^{\infty}$ denotes the asymptotic outage probability of x_i.

Proposition 1. *Based on the analytical results in* (9) *and* (10)*, when* $\rho \to \infty$*, the asymptotic outage probabilities of* x_l *for ipSIC/pSIC with* $e^{-x} \approx 1 - x$ *are given by*

$$P_{x_l,\infty}^{ipSIC} = 1 - \prod_{i=1}^{3} \lambda_i \left(\frac{\Phi_1 \Omega_l}{\Omega_l \lambda_1 + \beta_l} - \frac{\Phi_2 \Omega_l}{\Omega_l \lambda_2 + \beta_l} + \frac{\Phi_3 \Omega_l}{\Omega_l \lambda_3 + \beta_l} \right) \times \left[1 - \frac{\theta_l}{\Omega_k} - \frac{\varepsilon \tau \rho \Omega_I}{\Omega_k + \varepsilon \rho \tau \Omega_I} \left(1 - \frac{\theta_l \left(\Omega_k + \varepsilon \tau \rho \Omega_I\right)}{\tau \varepsilon \rho \Omega_I \Omega_k} \right) \right], \quad (15)$$

and

$$P_{x_l,\infty}^{pSIC} = 1 - \prod_{i=1}^{3} \lambda_i \left(\frac{\Phi_1 \Omega_l}{\Omega_l \lambda_1 + \beta_l} - \frac{\Phi_2 \Omega_l}{\Omega_l \lambda_2 + \beta_l} + \frac{\Phi_3 \Omega_l}{\Omega_l \lambda_3 + \beta_l} \right), \quad (16)$$

respectively. Substituting (15) *and* (16) *into* (14)*, the diversity orders of* x_l *with ipSIC/pSIC are equal to zeros.*

Remark 1. *An important conclusion from above analysis is that due to impact of residual interference, the diversity order of* x_l *with the use of ipSIC is zero. Additionally, the communication process of the first slot similar to uplink NOMA, even though under the condition of pSIC, diversity order is equal to zero as well for* x_l*. As can be observed that there are error floors for* x_l *with ipSIC/pSIC.*

Proposition 2. *Similar to the resolving process of* (15) *and* (16)*, the asymptotic outage probabilities of* x_t *with ipSIC/pSIC in high SNR regimes are given by*

$$P_{x_t,\infty}^{ipSIC} = 1 - \frac{\lambda_1' \lambda_2'}{\varphi_t \Omega_t \left(1 + \varepsilon \rho \beta_t \varphi_t \Omega_I\right)\left(\lambda_2' - \lambda_1'\right)} \times \left(\frac{\Omega_l}{\beta_l + \beta_t \Omega_1 \varphi_t + \Omega_l \lambda_1'} - \frac{\Omega_l}{\beta_l + \beta_t \Omega_1 \varphi_t + \Omega_l \lambda_2'} \right), \quad (17)$$

and

$$P_{x_t,\infty}^{pSIC} = 1 - \frac{\lambda_1' \lambda_2'}{\varphi_t \Omega_t \left(\lambda_2' - \lambda_1'\right)} \times \left(\frac{\Omega_l}{\beta_l + \beta_t \Omega_1 \varphi_t + \Omega_l \lambda_1'} - \frac{\Omega_l}{\beta_l + \beta_t \Omega_l \varphi_t + \Omega_l \lambda_2'} \right), \quad (18)$$

respectively. Substituting (17) *and* (18) *into* (14)*, the diversity orders of* x_t *for both ipSIC and pSIC are zeros.*

Remark 2. *Based on above analytical results of* x_l*, the diversity orders of* x_t *with ipSIC/pSIC are also equal to zeros. This is because residual interference is existent in the total communication process.*

4) Throughput Analysis: In delay-limited transmission scenario, the BS transmits message to users at a fixed rate, where system throughput will be subject to wireless fading channels. Hence the corresponding throughput of TWR-NOMA with ipSIC/pSIC is calculated as [7]

$$R_{dl}^{\psi} = \left(1 - P_{x_1}^{\psi}\right) R_{x_1} + \left(1 - P_{x_2}^{\psi}\right) R_{x_2} + \left(1 - P_{x_3}^{\psi}\right) R_{x_3} + \left(1 - P_{x_4}^{\psi}\right) R_{x_4}, \quad (19)$$

TABLE I: Table of Parameters for Numerical Results

Monte Carlo simulations repeated	10^6 iterations
Power allocation coefficients of NOMA	$b_1 = b_3 = 0.2$ $b_2 = b_4 = 0.8$
Targeted data rates	$R_1 = R_3 = 0.1$ BPCU $R_2 = R_4 = 0.01$ BPCU
Pass loss exponent	$\alpha = 2$
The distance between R and D_1 or D_3	$d_1 = 2$ m
The distance between R and D_2 or D_4	$d_2 = 10$ m

where $\psi \in (ipSIC, pSIC)$. $P_{x_1}^{\psi}$ and $P_{x_3}^{\psi}$ with ipSIC/pSIC can be obtained from (9) and (10), respectively, while $P_{x_2}^{\psi}$ and $P_{x_4}^{\psi}$ with ipSIC/pSIC can be obtained from (12) and (13), respectively.

IV. Numerical Results

In this section, numerical results are provide to investigate the impact levels of IS on outage probability for TWR-NOMA systems. The simulation parameters used are summarized in Table I, where BPCU is short for bit per channel use. Due to the reciprocity of channels between G_1 and G_2, the outage behaviors of x_1 and x_2 in G_1 are presented to illustrate availability of TWR-NOMA. Without loss of generality, the power allocation coefficients of x_1 and x_2 are set as $a_1 = 0.8$ and $a_2 = 0.2$, respectively. Ω_1 and Ω_2 are set to be $\Omega_1 = d_1^{-\alpha}$ and $\Omega_2 = d_2^{-\alpha}$, respectively.

A. Outage Probability

Fig. 1 plots the outage probabilities of x_1 and x_2 with both ipSIC and pSIC versus SNR for simulation setting with $\varpi_1 = \varpi_2 = 0.01$ and $\Omega_I = -20$ dB. The solid and dashed curves represent the exact theoretical performance of x_1 and x_2 for both ipSIC and pSIC, corresponding to the results derived in (9), (10) and (12), (13), respectively. Apparently, the outage probability curves match perfectly with Monte Carlo simulation results. As can be observed from the figure, the outage behaviors of x_1 and x_2 for TWR-NOMA are superior to TWR-OMA in the low SNR regime. This is due to the fact that the influence of IS is not the dominant factor at low SNR. Furthermore, another observation is that the pSIC is capable of enhancing the performance of NOMA compare to the ipSIC. In addition, the asymptotic curves of x_1 and x_2 with ipSIC/pSIC are plotted according to (15), (16) and (17), (16), respectively. It can be seen that the outage behaviors of x_1 and x_2 converge to the error floors in the high SNR regime. The reason can be explained that due to the impact of residual interference by the use of ipSIC, x_1 and x_2 result in zero diversity orders. Although the pSIC is carried out in TWR-NOMA system, x_1 and x_2 also obtain zero diversity orders. This is due to the fact that when the relay first detect the strongest signal in the first slot, it will suffer interference from the weaker signal. This observation verifies the conclusion **Remark 1** in Section III.

Fig. 2 plots the outage probabilities of x_1 and x_2 versus SNR with the different impact levels of IS from $\varpi_1 = \varpi_2 = 0$ to $\varpi_1 = \varpi_2 = 0.1$. The solid and dashed curves represent the outage behaviors of x_1 and x_2 with ipSIC/pSIC, respectively.

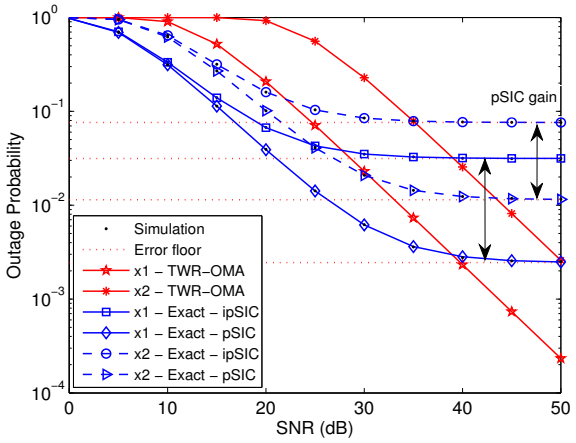

Fig. 1: Outage probability versus the transmit SNR.

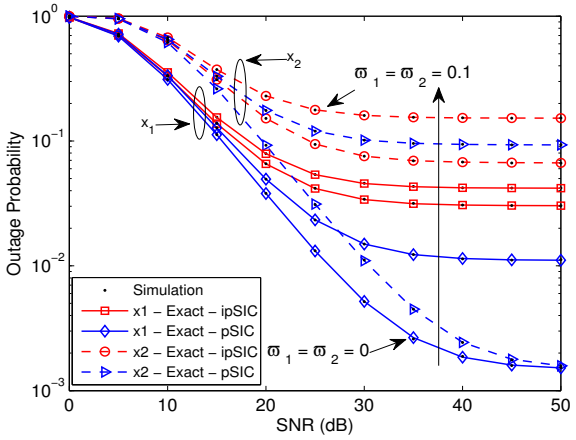

Fig. 2: Outage probability versus the transmit SNR, with $\Omega_I = -20$ dB.

As can be seen that when the impact level of IS is set to be $\varpi_1 = \varpi_2 = 0$, there is no IS between A_1 and A_2 at the relay, which can be viewed as a benchmark. Additionally, one can observed that with the impact levels of IS increasing, the outage performance of TWR-NOMA system degrades significantly. Hence it is crucial to hunt for efficient strategies for suppressing the effect of interference between antennas. Fig. 3 plots the outage probability versus SNR with different values of residual IS from -20 dB to 0 dB. It can be seen that the different values of residual IS affects the performance of ipSIC seriously. Similarly, as the values of residual IS increases, the preponderance of ipSIC is inexistent. When $\Omega_I = 0$ dB, the outage probability of x_1 and x_2 will be in close proximity to one. Therefore, it is important to design effective SIC schemes for TWR-NOMA.

Fig. 4 plots system throughput versus SNR in delay-limited transmission mode for TWR-NOMA with different values of residual IS from -20 dB to -10 dB. The blue solid curves represent throughput for TWR-NOMA with both pSIC and

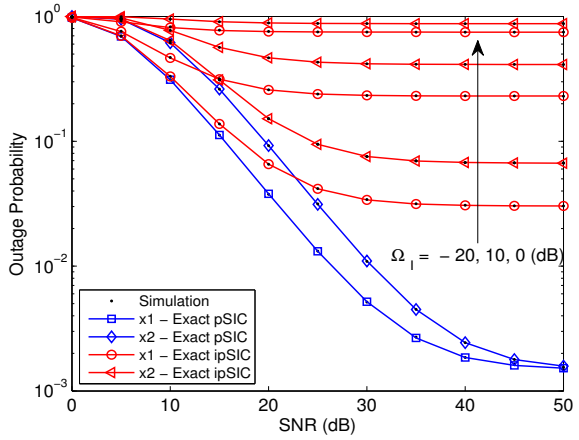

Fig. 3: Outage probability versus the transmit SNR, with $\varpi_1 = \varpi_2 = 0$.

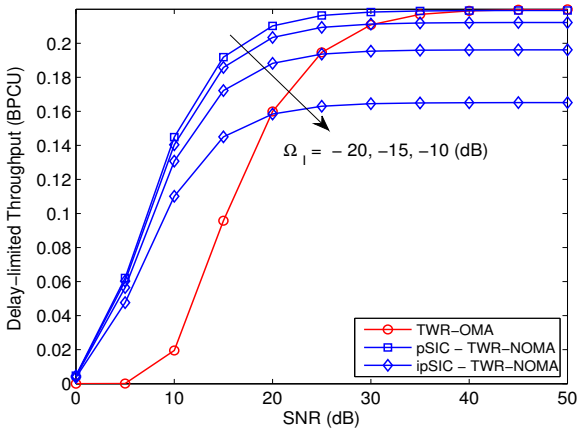

Fig. 4: System throughput in delay-limited transmission mode versus SNR with ipSIC/pSIC, $\varpi_1 = \varpi_2 = 0.01$.

ipSIC, which can be obtained from (19). One can observe that TWR-NOMA is capable of achieving a higher throughput compared to TWR-OMA in the low SNR regime, since it has a lower outage probability. Moreover, the figure confirms that TWR-NOMA converges to the throughput ceiling in high SNR regimes. It is worth noting that ipSIC considered for TWR-NOMA will further degrade throughput with the values of residual IS becomes larger in high SNR regimes.

V. Conclusion

This paper has investigated the application of TWR to NOMA systems, in which two pairs of users can exchange their information between each other by the virtue of a relay node. The performance of TWR-NOMA has been characterized in terms of outage probability and ergodic rate for both ipSIC and pSIC. Furthermore, the closed-form expressions of outage probability for the NOMA users' signals have been derived. Owing to the impact of IS at relay, there were the error floors for TWR-NOMA with ipSIC/pSIC in high SNR regimes and zero diversity orders were obtained. Based on the analytical results, it was shown that the performance of TWR-NOMA with ipSIC/pSIC outperforms TWR-OMA in the low SNR regime.

Appendix A: Proof of Theorem 1

Substituting (3), (5) and (6) into (8), the outage probability of x_l can be further given by

$$P_{x_l}^{ipSIC} = 1 - \underbrace{\Pr\left(\frac{\rho|h_l|^2 a_l}{\rho|h_t|^2 a_t + \rho\varpi_1(|h_k|^2 a_k + |h_r|^2 a_r) + 1} > \gamma_{th_l}\right)}_{J_1} \times \underbrace{\Pr\left(\frac{\rho|h_k|^2 b_t}{\rho|h_k|^2 b_l + \rho\varpi_2|h_k|^2 + 1} > \gamma_{th_t}, \frac{\rho|h_k|^2 b_l}{\varepsilon\rho|g|^2 + \rho\varpi_2|h_k|^2 + 1} > \gamma_{th_l}\right)}_{J_2}, \quad (A.1)$$

where $\varepsilon = 1$.

To calculate the probability J_1 in (A.1), let $Z = \rho a_t|h_t|^2 + \rho\varpi_1 a_k|h_k|^2 + \rho\varpi_1 a_r|h_r|^2$. We first calculate the PDF of Z and then give the process derived of J_1. As is known, $|h_i|^2$ follows the exponential distribution with the means Ω_i, $i \in (1,2,3,4)$. Furthermore, we denote that $Z_1 = \rho a_t|h_t|^2$, $Z_2 = \rho\varpi_1 a_k|h_k|^2$ and $Z_3 = \rho\varpi_1 a_r|h_r|^2$ are also independent exponentially distributed random variables (RVs) with means $\lambda_1 = \frac{1}{\rho a_t \Omega_t}$, $\lambda_2 = \frac{1}{\rho\varpi_1 a_k \Omega_k}$ and $\lambda_3 = \frac{1}{\rho\varpi_1 a_r \Omega_r}$, respectively. Based on [18], for the independent non-identical distributed (i.n.d) fading scenario, the PDF of Z can be given by

$$f_Z(z) = \prod_{i=1}^{3}\lambda_i\left(\Phi_1 e^{-\lambda_1 z} - \Phi_2 e^{-\lambda_2 z} + \Phi_3 e^{-\lambda_3 z}\right), \quad (A.2)$$

where $\Phi_1 = \frac{1}{(\lambda_2-\lambda_1)(\lambda_3-\lambda_1)}$, $\Phi_2 = \frac{1}{(\lambda_3-\lambda_2)(\lambda_2-\lambda_1)}$ and $\Phi_3 = \frac{1}{(\lambda_3-\lambda_1)(\lambda_3-\lambda_2)}$.

According to the above explanations, J_1 is calculated as follows:

$$J_1 = \Pr\left(|h_l|^2 > (Z+1)\beta_l\right) = \int_0^\infty f_Z(z) e^{-\frac{(z+1)\beta_l}{\Omega_l}} dz. \quad (A.3)$$

Substituting (A.2) into (A.3) and after some algebraic manipulations, J_1 is given by

$$J_1 = e^{-\frac{\beta_l}{\Omega_l}}\prod_{i=1}^{3}\lambda_i\left(\frac{\Phi_1\Omega_l}{\Omega_l\lambda_1+\beta_l} - \frac{\Phi_2\Omega_l}{\Omega_l\lambda_2+\beta_l} + \frac{\Phi_3\Omega_l}{\Omega_l\lambda_3+\beta_l}\right), \quad (A.4)$$

where $\beta_l = \frac{\gamma_{th_l}}{\rho a_l}$.

J_2 can be further calculated as follows:

$$J_2 = \Pr\left(|h_k|^2 > \max(\tau_l, \xi_t) \triangleq \theta_l, |g|^2 < \frac{|h_k|^2 - \tau_l}{\varepsilon\rho\tau_l}\right)$$

$$= \int_{\theta}^{\infty} \frac{1}{\Omega_k} \left(e^{-\frac{y}{\Omega_k}} - e^{-\frac{y-\tau_l}{\varepsilon \tau_l \rho \Omega_I} - \frac{y}{\Omega_k}} \right) dy$$
$$= e^{-\frac{\theta_l}{\Omega_k}} - \frac{\tau_l \varepsilon \rho \Omega_I}{\Omega_k + \varepsilon \rho \tau_l \Omega_I} e^{-\frac{\theta_l (\Omega_k + \rho \tau_l \varepsilon \Omega_I)}{\tau_l \varepsilon \rho \Omega_I \Omega_k} + \frac{1}{\varepsilon \rho \Omega_I}}, \quad \text{(A.5)}$$

where $\xi_t = \frac{\gamma_{th_t}}{\rho\left(b_t - b_l \gamma_{th_t} - \varpi_2 \gamma_{th_t}\right)}$ with $b_t > (b_l + \varpi_2)\gamma_{th_t}$, $\tau_l = \frac{\gamma_{th_l}}{\rho\left(b_l - \varpi_2 \gamma_{th_l}\right)}$ with $b_l > \varpi_2 \gamma_{th_l}$. Combining (A.4) and (A.5), we can obtain (9). The proof is complete.

Appendix B: Proof of Theorem 2

Substituting (3), (4), (6) and (7) into (11), the outage probability of x_t is rewritten as

$$P_{x_t}^{ipSIC} = 1 - \underbrace{\Pr\left(\frac{\rho |h_t|^2 a_t}{\varepsilon \rho |g|^2 + \rho \varpi_1 (|h_k|^2 a_k + |h_r|^2 a_r) + 1} > \gamma_{th_t}, \frac{\rho |h_l|^2 a_l}{\rho |h_t|^2 a_t + \rho \varpi_1 (|h_k|^2 a_k + |h_r|^2 a_r) + 1} > \gamma_{th_l} \right)}_{\Theta_1} \times \underbrace{\Pr\left(\frac{\rho |h_k|^2 b_t}{\rho |h_k|^2 b_l + \rho \varpi_2 |h_k|^2 + 1} > \gamma_{th_t} \right)}_{\Theta_2} \times \underbrace{\Pr\left(\frac{\rho |h_r|^2 b_t}{\rho |h_r|^2 b_l + \rho \varpi_2 |h_r|^2 + 1} > \gamma_{th_t} \right)}_{\Theta_3}, \quad \text{(B.1)}$$

where $\varpi_1 = \varpi_2 \in [0, 1]$ and $\varepsilon = 1$.

Similar to (A.2), let $Z' = \rho \varpi_1 a_k |h_k|^2 + \rho \varpi_1 a_r |h_r|^2$, the PDF of Z' is given by

$$f_{Z'}\left(z'\right) = \prod_{i=1}^{2} \lambda_i' \left(\frac{e^{-\lambda_1' z'}}{\left(\lambda_2' - \lambda_1'\right)} - \frac{e^{-\lambda_2' z'}}{\left(\lambda_2' - \lambda_1'\right)} \right), \quad \text{(B.2)}$$

where $\lambda_1' = \frac{1}{\rho \varpi_1 a_k \Omega_k}$ and $\lambda_2' = \frac{1}{\rho \varpi_1 a_r \Omega_r}$.

After some variable substitutions and manipulations,

$$\Theta_1 = \Pr\left(|h_t|^2 > \beta_t \left(\varepsilon \rho |g|^2 + Z' + 1 \right), |h_l|^2 > \beta_l \left(\rho |h_t|^2 a_t + Z' + 1 \right) \right) = \frac{1}{\varphi_t \Omega_t \left(1 + \varepsilon \rho \beta_t \varphi_t \Omega_I\right)} e^{-\frac{\beta_l}{\Omega_1} - \beta_t \varphi_t} \times \int_0^{\infty} f_{Z'}\left(z'\right) e^{-\frac{\left(\beta_l + \beta_t \Omega_l \varphi_t\right) z'}{\Omega_l}} dx, \quad \text{(B.3)}$$

where $\beta_t = \frac{\gamma_{th_t}}{\rho a_t}$ and $\varphi_t = \frac{\Omega_l + \rho \beta_l a_t \Omega_t}{\Omega_l \Omega_t}$.

Substituting (B.2) into (B.3), Θ_1 can be given by

$$\Theta_1 = \frac{e^{-\frac{\beta_l}{\Omega_l} - \beta_t \varphi_t}}{\varphi_t \Omega_t \left(1 + \beta_t \varepsilon \rho \varphi_t \Omega_I\right) \left(\lambda_2' - \lambda_1'\right)} \times \prod_{i=1}^{2} \lambda_i' \left(\frac{\Omega_l}{\beta_l + \beta_t \Omega_l \varphi_t + \Omega_l \lambda_1'} - \frac{\Omega_l}{\beta_l + \beta_t \Omega_l \varphi_t + \Omega_l \lambda_2'} \right). \quad \text{(B.4)}$$

Θ_2 and Θ_3 can be easily calculated

$$\Theta_2 = \Pr\left(|h_k|^2 > \xi_t \right) = e^{-\frac{\xi_t}{\Omega_k}}, \quad \text{(B.5)}$$

and

$$\Theta_3 = \Pr\left(|h_r|^2 > \xi_t \right) = e^{-\frac{\xi_t}{\Omega_r}}, \quad \text{(B.6)}$$

respectively, where $\xi_t = \frac{\gamma_{th_t}}{\rho\left(b_t - b_l \gamma_{th_t} - \varpi_2 \gamma_{th_t}\right)}$ with $b_t > (b_l + \varpi_2)\gamma_{th_t}$.

Finally, combining (B.4), (B.5) and (B.6), we can obtain (12). The proof is complete.

References

[1] Y. Liu, Z. Qin, M. Elkashlan, Z. Ding, A. Nallanathan, and L. Hanzo, "Nonorthogonal multiple access for 5G and beyond," *Proceedings of the IEEE*, vol. 105, no. 12, pp. 2347–2381, Dec. 2017.

[2] Z. Ding, Y. Liu, J. Choi, Q. Sun, M. Elkashlan, C. L. I, and H. V. Poor, "Application of non-orthogonal multiple access in LTE and 5G networks," *IEEE Commun. Mag.*, vol. 55, no. 2, pp. 185–191, Feb. 2017.

[3] S. M. R. Islam, N. Avazov, O. A. Dobre, and K. s. Kwak, "Power-domain non-orthogonal multiple access (noma) in 5G systems: Potentials and challenges," *IEEE Commun. Surveys. Tutorials*, vol. 19, no. 2, pp. 721–742, Sec. 2017.

[4] Y. Cai, Z. Qin, F. Cui, G. Y. Li, and J. A. McCann, "Modulation and multiple access for 5G networks," *IEEE Commun. Surveys. Tutorials*, vol. PP, no. 99, pp. 1–1, 2017.

[5] T. M. Cover and J. A. Thomas, *Elements of information theory*, 6th ed., Wiley and Sons, New York, 1991.

[6] Z. Ding, M. Peng, and H. V. Poor, "Cooperative non-orthogonal multiple access in 5G systems," *IEEE Commun. Lett.*, vol. 19, no. 8, pp. 1462–1465, Aug. 2015.

[7] Y. Liu, Z. Ding, M. Elkashlan, and H. V. Poor, "Cooperative non-orthogonal multiple access with simultaneous wireless information and power transfer," *IEEE J. Sel. Areas Commun.*, vol. 34, no. 4, pp. 938–953, Apr. 2016.

[8] J. Men, J. Ge, and C. Zhang, "Performance analysis of non-orthogonal multiple access for relaying networks over Nakagami-m fading channels," *IEEE Trans. Veh. Technol.*, to appear in 2016.

[9] X. Yue, Y. Liu, S. Kang, A. Nallanathan, and Z. Ding, "Outage performance of full/half-duplex user relaying in NOMA systems," in *IEEE Proc. of International Commun. Conf. (ICC)*, Paris, FRA, May. 2017, pp. 1–6.

[10] C. E. Shannon, "Two-way communication channels," *in Proc. 4th Berkeley Symp. Math. Stat and Prob.*, vol. 1, pp. 611–644, 1961.

[11] A. Hyadi, M. Benjillali, and M. S. Alouini, "Outage performance of decode-and-forward in two-way relaying with outdated CSI," *IEEE Trans. Veh. Technol.*, vol. 64, no. 12, pp. 5940–5947, Dec. 2015.

[12] C. Li, B. Xia, S. Shao, Z. Chen, and Y. Tang, "Multi-user scheduling of the full-duplex enabled two-way relay systems," *IEEE Trans. Wireless Commun.*, vol. 16, no. 2, pp. 1094–1106, Feb. 2017.

[13] Z. Ding, Z. Yang, P. Fan, and H. V. Poor, "On the performance of non-orthogonal multiple access in 5G systems with randomly deployed users," *IEEE Signal Process. Lett.*, vol. 21, no. 12, pp. 1501–1505, Dec. 2014.

[14] Y. Liu, Z. Qin, M. Elkashlan, A. Nallanathan, and J. A. McCann, "Non-orthogonal multiple access in large-scale heterogeneous networks," *IEEE J. Sel. Areas Commun.*, vol. 35, no. 12, pp. 2667–2680, Dec. 2017.

[15] M. F. Kader, M. B. Shahab, and S. Y. Shin, "Exploiting non-orthogonal multiple access in cooperative relay sharing," *IEEE Commun. Lett.*, to appear in 2017.

[16] Y. Liu, Z. Ding, M. Elkashlan, and J. Yuan, "Non-orthogonal multiple access in large-scale underlay cognitive radio networks," *IEEE Trans. Veh. Technol.*, vol. 65, no. 12, pp. 10 152–10 157, Dec. 2016.

[17] Y. Liu, Z. Qin, M. Elkashlan, Y. Gao, and L. Hanzo, "Enhancing the physical layer security of non-orthogonal multiple access in large-scale networks," *IEEE Trans. Wireless Commun.*, vol. 16, no. 3, pp. 1656–1672, Mar. 2017.

[18] S. Nadarajah, "A review of results on sums of random variables," *Acta Appl. Math.*, vol. 103, no. 2, pp. 131–141, Sep. 2008.